

## Electrical Properties of Thin Iron Films Grown on Clean Si(100) and on Si(100)-c(4×12)-Al Surface Phase\*

Dmitry L. Goroshko,<sup>†</sup> Nikolay G. Galkin, and Alexander S. Gournik

*Institute for Automation and Control Processes,  
Far Eastern Branch of Russian Academy of Sciences,  
5 Radio Str., Vladivostok, 690041, Russia*

(Received 29 December 2008; Accepted 19 January 2009; Published 14 March 2009)

Electrical properties of thin iron films deposited at room temperature both on clean Si(100) and prefabricated surface phase Si(100)-c(4×12)-Al were studied by means of *in situ* Hall effect registration and conductance measurements. It was shown that Si(100)-c(4×12)-Al surface phase blocks intermixing of iron and substrate atoms. Conductance and mobility of the majority carriers in this surface phase is higher than that in Si(100)2×1 within the temperature range from room temperature to 180°C. Deposition of less than 25 monolayers of iron on the clean Si(100) resulted in significant reduction of conductance. Continuous iron film on Si(100)-c(4×12)-Al forms at coverage approximately twice thinner compared to deposition on Si(100)2×1.

[DOI: 10.1380/ejsnt.2009.167]

Keywords: Diffusion; Conductivity; Electrical transport; Iron; Si(100)

### I. INTRODUCTION

It has been shown in multiple works that upon deposition of iron on Si(100) at room temperature (RT), some Fe-Si mixture forms at the early stage and further deposition results in formation of randomly oriented iron crystals [1, 2]. In production of spin-electron devices, a difficult task is creation of a buffer layer blocking formation of silicide at the early stages of iron deposition [3]. As well, the Fe/Si interface problem arises in growing ultra-thin magnetic films on semiconductors [4].

Many works has been devoted to creation of a sharp border Fe-Si; their main idea being passivation of the silicon surface. In Ref. [5, 6] the authors applied modification of silicon surface by Sb and H. In Ref. [7] a template technique was used to prevent the formation of disordered interfacial iron silicides. But the buffer layer itself was 1 nm-thick.

Usage of appropriate surface phases (SP) as diffusion barrier seems very perspective since their thickness does not exceed a few atomic layers. In Ref. [8] it was demonstrated that the SP CrSi<sub>2</sub> is a good diffusion barrier reducing Fe-Si intermixing.

In this work the SP Si(100)-c(4×12)-Al is used as a diffusion barrier. The good feature of this SP is its thermal stability up to 800°C [9]. That allows not only to grow epitaxial films at RT upon this SP but to form iron silicides at higher temperatures.

Despite initial stages of iron film growth on the surface Si(100)2×1 at RT has been studied in many works, the data on electric properties of this system, for the authors' knowledge, is absent. The results of Hall measurements of iron film grown on Si(100)-c(4×12)-Al SP are compared to those for the iron films grown on the clean surface Si(100).

\*This paper was presented at the 8th Japan-Russia Seminar on Semiconductor Surfaces (JRSSS-8), Tohoku University, Japan, 19-23 October, 2008.

<sup>†</sup>Corresponding author: goroshko@iacp.dvo.ru

### II. EXPERIMENTAL

Experiments were carried out in the ultra-high vacuum (UHV) chamber with the base vacuum of  $1 \times 10^{-9}$  Torr equipped with low energy electron diffraction (LEED) analyzer, UHV 6-probe Hall measurement unit [10], sublimation sources of Fe and Al. 4.5 Ohm-cm *p*-type Si(100) ribbons with dimensions of  $15 \times 5 \times 0.35$  mm<sup>3</sup> were used as substrates. Before loading into the UHV chamber, the samples were chemically cleaned. Under UHV conditions the samples were degassed at 600°C during 10 hours. After cooling for 12 hours, the samples were cleaned by a series of flashes at 1200°C. As a result of this procedure, a bright LEED pattern corresponding to Si(100)2×1 was observed.

Aluminum was deposited from an Al-covered tungsten spiral heated by AC current. The Si(100)-c(4×12)-Al surface phase was obtained using evaporation of about 1 ML of Al (a saturation coverage) onto the hot Si(100)2×1 surface (T=700-800°C). Iron (99.9%) was deposited from an Fe-coated tungsten wire. The deposition rate was  $\approx 1$  ML/min. Both Al and Fe deposition rates were calibrated by a quartz microbalance. Iron was deposited at small portions onto the clean silicon surface or the prefabricated SP Si(100)-c(4×12)-Al at RT. After each deposition, the Hall voltage  $U_H$  and the longitudinal voltage  $U_\rho$  (proportional to the resistance) were measured by our original unit [10]. The surface morphology was studied by ex-situ atomic force microscope (AFM) Solver P47 immediately after the samples were unloaded from the UHV chamber. Contact and tapping modes were used.

### III. RESULTS

The LEED patterns of the surfaces before iron deposition are given in Fig. 1. Figure 1(a) shows the two-domain phase Si(100)2×1 formed by high temperature annealing of the surface Si(100). Sharp spots and absence of the background evidence good quality of the surface. The LEED pattern presented in Fig. 1(b) was obtained from

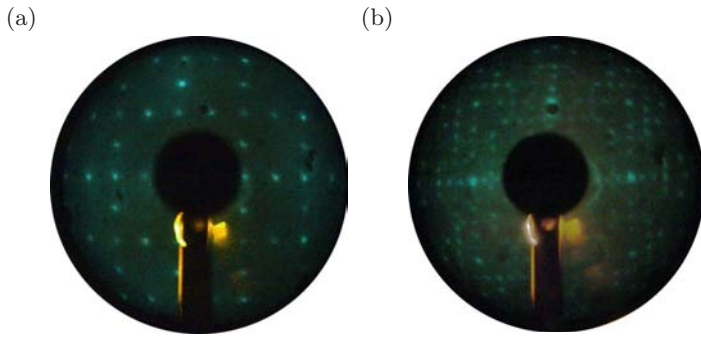


FIG. 1: LEED patterns from the atomically-clean surface Si(100) (a) and SP Si(100)-c(4×12)-Al (b).

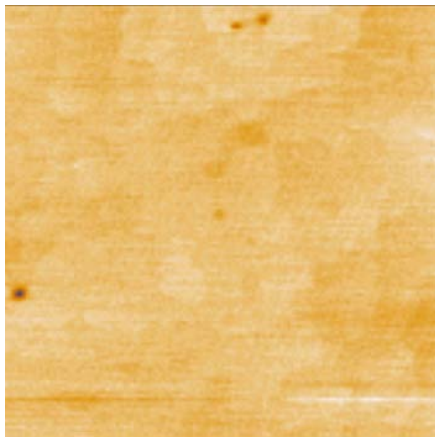


FIG. 2: A 1.2×1.2μm<sup>2</sup> AFM image of the silicon sample with SP Si(100)-c(4×12)-Al.

the Si(100)-(4×12)-Al surface just after this SP had been formed. The spots characteristic for this SP are clearly seen.

In order to check the morphology of the SP Si(100)-c(4×12)-Al, special AFM study of an analogous sample with this SP was carried out. The AFM picture of this surface is given in Fig. 2. It is seen that the surface is smooth (mean square roughness is about 0.14 nm) and has not any defects visible by the AFM.

The Hall voltage  $U_H$  and longitudinal voltage  $U_\rho$  are plotted in Fig. 3 versus the thickness of the iron deposited both for the clean Si(100)2×1 surface and pre-fabricated SP Si(100)-c(4×12)-Al. The error bars given on the curves represent the mean square errors for the results measured a few times at the same iron thickness. The reason for that is as follows. In our original Hall measurement unit [10] the head with 6 probes pressed to the sample surface is used. To carry out a series of deposition-measurement procedures, the sample has to be rotated many times between the evaporation and measurement positions. The results of the measurements can slightly differ after each landing of the probes on the surface. For this reason, for each portion of iron the cycles of 3-4 landing/measurement procedure were carried out and the results averaged. It is seen that both the  $U_H$  and  $U_\rho$  errors for such cycles do not exceed 5% for the worst case.

It is obvious that the dependencies of the Hall voltage

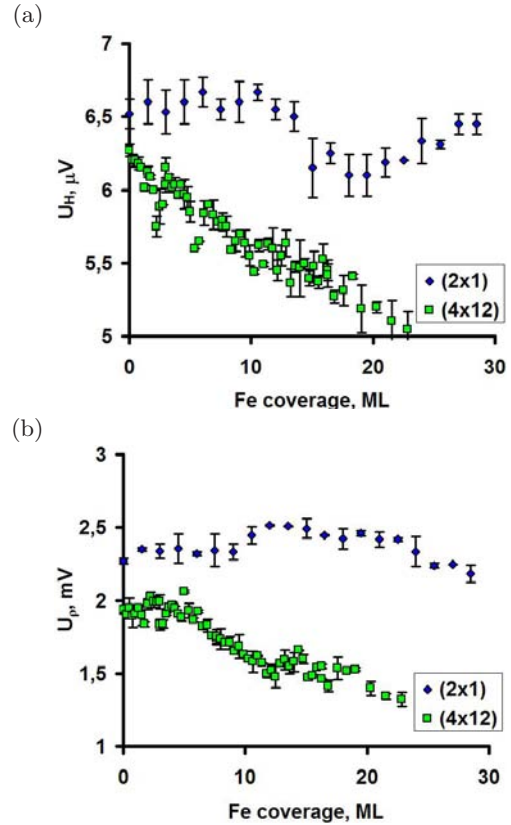


FIG. 3: Dependence of Hall voltage  $U_H$  (a) and longitudinal voltage  $U_\rho$  (b) on iron coverage. Rhombuses and squares correspond to the results measured for the Si(100)2×1 surface and SP Si(100)-c(4×12)-Al, respectively.

on iron thickness significantly differ for the two different surfaces (Fig. 3(a)). That indicates serious difference in the growth process. The Hall voltage for the clean surface, taking into account the measurement errors, is practically constant up to  $d_{Fe} \sim 12$  ML then it slightly decreases by  $\sim 5\%$ . From  $d_{Fe} \sim 20$  ML some increase of  $U_H$  is seen and at 29 ML it reaches the same value as at the beginning of iron deposition. For the SP Si(100)-c(4×12)-Al surface,  $U_H$  decreases monotonically within the whole range of iron coverage studied except two sharp negative peaks at 2.25 ML and 5.5 ML which cannot be attributed to measurement errors. The nature of these peaks is not clear and they are not discussed in this work.

The values  $U_\rho$  for the two types of samples also differ significantly (Fig. 3(b)). For the case of clean Si(100) increasing of  $U_\rho$  was noticed right after deposition of the first iron portion. The next increase by 8% occurred from 10 ML to 12 ML. After that a gradual decrease of  $U_\rho$  for the range from 12 ML up to 29 ML was observed. For the Si(100)-c(4×12)-Al surface,  $U_\rho$  is constant for  $d_{Fe} \leq 5$ ML, then it falls by  $\sim 25\%$  for  $5 \text{ ML} \leq d_{Fe} \leq 12 \text{ ML}$ ; upon further iron deposition up to 23 ML the decrease of  $U_\rho$  slows down.

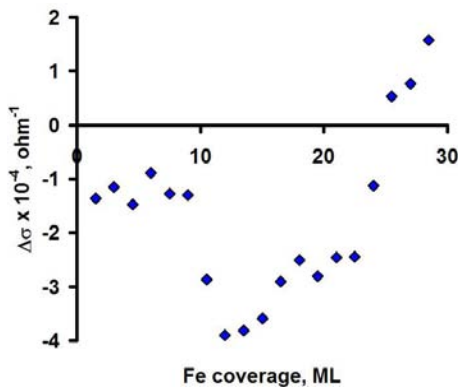


FIG. 4: Relative variations of the sample conductance versus iron coverage for the deposition on clean Si(100)2×1. The conductance of the Si(100)2×1 is taken for the initial level.

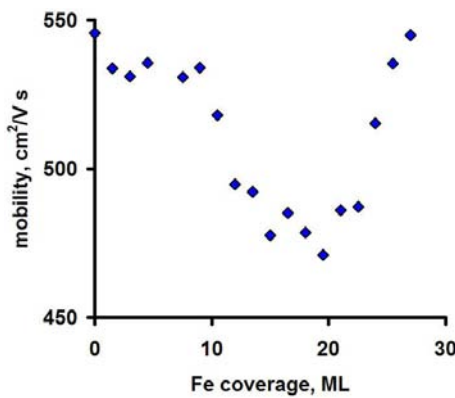


FIG. 5: Dependence of the effective mobility of holes on iron coverage for Fe/Si(100).

IV. DISCUSSIONS

The measured voltages  $U_H$  and  $U_\rho$  are some effective values including contributions from the bulk, the space charge layer and surface states zone. For this reason, interpretation of their behavior is a complicated problem. It was shown in Ref. [11] that, to separate the surface-related contributions, the distance between the probes should be reduced down to nanoscale distance. Taking into account the distance between measuring probes in our case is 5 or 10 mm and the sample is 0.35mm thick, it is clear that the contribution from the bulk is large. Nevertheless, qualitatively, we can guess that only the contributions of the topmost layers of the sample are significantly affected by iron deposition but the bulk stays intact. Hence, the variations of the measured values can be attributed to the film and surface-nearest layers of the sample.

A. Conductance of thin disordered iron films on the clean surface Si(100)

Figure 4 presents the variations of conductance versus iron coverage for the system Fe/Si(100). It is seen that the conductance falls sharply (by 3.4%) after deposition of the very first portion of iron. The conductance remains

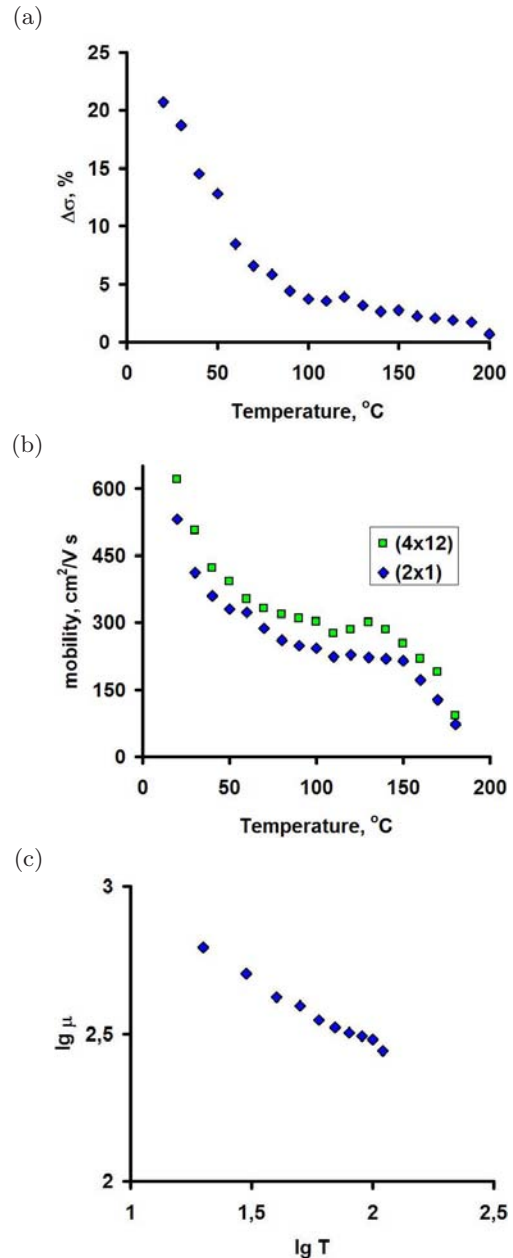


FIG. 6: (a) Relative change of the conductance in the sample with SP Si(100)-c(4×12)-Al versus temperature. The conductance of the sample Si(100)2×1 is used as the reference. (b) Hole mobility dependence on temperature in the clean silicon (rhombuses) and the sample with SP Si(100)-c(4×12)-Al (squares). (c) The dependence (a) plotted in the logarithm scale.

nearly constant for  $d_{Fe} \leq 9$  ML, in the range (9-12) ML it reduces by ~10% and then, for  $12 \text{ ML} \leq d_{Fe} \leq 29 \text{ ML}$ , it increases.

The shape of the plot agrees qualitatively with the admitted now model of disordered iron film formation on atomically-clean Si(100). In Ref. [12] it was shown by XPS that, for RT iron deposition, within the range  $1 \text{ ML} \leq d_{Fe} \leq 5 \text{ ML}$  a new phase is formed representing a solid Fe-Si solution which, for  $d_{Fe} > 5 \text{ ML}$  (critical value) transforms into Fe-rich silicide  $Fe_3Si$ . Existence of a critical coverage has been proved in other works as well.

The shape of the plot in Fig. 4 also demonstrates three

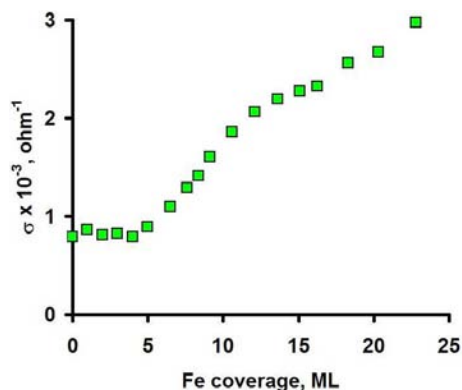


FIG. 7: Dependence of conductance change on Fe coverage in the system Fe film/SP Si(100)-c(4×12)-Al/silicon substrate.

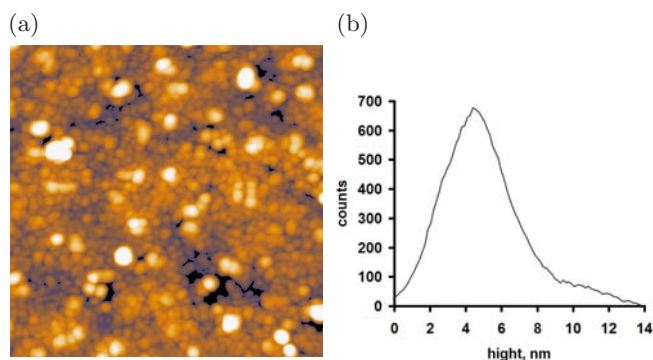


FIG. 8: (a) A  $1.9 \times 1.9 \mu\text{m}^2$  atomic force image of the sample with 23 ML iron deposited upon the prefabricated SP Si(100)-c(4×12)-Al. (b) Histogram of height distribution for the sample surface.

stages of the film growth but the critical value in our case is 9 ML and the iron film begins to form upon a silicide when the coverage reaches 12 ML. For this reason we see decrease of hole mobility (Fig. 5) caused at first by carrier scattering in the layer of Fe-Si mixture (0-10 ML) and then in Fe<sub>3</sub>Si (10-20 ML). It seems reasonable to guess that the increase of the mobility for  $22 \text{ ML} \leq d_{\text{Fe}} \leq 29 \text{ ML}$  is related to formation of a continuous film which begins to form at 20 ML, as seen in Fig. 4. The conductance calculated from the slope of the plot in the range of 22-29 ML (see Fig. 4) yields  $7.5 \times 10^3 (\text{Ohm}\cdot\text{cm})^{-1}$  which is smaller than that for pure iron by the factor of 13. It is explained by carriers scattering in the film due to crystal structure defects.

### B. Electro-physical properties of the surface phase Si(100)-c(4×12)-Al

In order to make our analysis of the surface phase Si(100)-c(4×12)-Al properties more comprehensive, the measurements were carried out not only at RT but at increased temperature as well.

The calculations based on the results of the Hall measurements show that the main carriers in this system are holes. It was shown that the conductance of this SP is

higher than that of the clean silicon both at RT and elevated temperatures (see Fig. 6(a)) which is in agreement with the existing data [13]. For RT this difference is 18%.

It was found that the hole mobility in the sample with the SP is higher than that in the clean sample within the whole temperature range studied. At RT the hole mobility in the sample with the SP is  $620 \text{ cm}^2/\text{V}\cdot\text{s}$  which is 17% higher than that for the Si(100)2×1 sample (see Fig. 6(b)).

Mobility of the majority carriers vs. temperature can be presented as  $\mu_{\text{H}}(T) = \mu_{\text{H}}(T/T_0)^\alpha$ , whence exponent  $\alpha$  appears  $\alpha = \Delta \lg \mu_{\text{H}} / \Delta \lg T$ . Based on  $\alpha$  one can deduce the carrier scattering mechanism which is complex in semiconductors. It includes a few contributions related to phonons ( $\alpha = -3/2$ ), neutral impurities ( $\alpha = 0$ ), dislocations ( $\alpha = 1$ ) and ionized impurities ( $\alpha = 3/2$ ). Nevertheless, on the basis of the mobility versus temperature plot (Fig. 6(c)) we can say that scattering for the sample with SP (the effective exponent  $\alpha = -0.46$ ) is mainly originated from dissipation on neutral impurities and phonons.

The observed increase in the hole mobility which is a consequence of the decrease of scattering resulted in increasing of conductance can be explained by change in the energy zones bending as a result of saturation of the silicon atoms' dangling bonds by aluminum atoms in the SP Si(100)-c(4×12)-Al.

### C. Conductance of Si(100)-c(4×12)-Al with iron film deposited on it

The results of the Hall measurements show that, like for the system SP Si(100)-c(4×12)-Al/silicon substrate, the main carriers in the system Fe film/SP Si(100)-c(4×12)-Al/substrate are holes. Their effective mobility gradually varied from  $620 \text{ cm}^2/\text{V}\cdot\text{s}$  (before Fe deposition) up to  $725 \text{ cm}^2/\text{V}\cdot\text{s}$  (for Fe coverage of 23 ML). The hole concentration increased monotonically with Fe coverage from  $1.36 \times 10^{15} \text{ cm}^{-3}$  up to  $1.7 \times 10^{15} \text{ cm}^{-3}$ .

Conductance variations for the case of iron growth upon the Al SP prefabricated on Si(100) substrate are presented in Fig. 7. No changes in the conductance are seen at the initial stage of growth (below 4 ML). Beginning from  $d_{\text{Fe}} = 4 \text{ ML}$ , the conductance monotonically grow. Some peculiarity and decrease of the slope are clearly seen near the coverage of 12 ML. It is noteworthy, such a behavior of the curve differs from that reported in Ref. [13] for Al or In deposition upon the SP Si(100)-c(4×12)-Al where the conductance of the system metal/Si(100)-c(4×12)-Al/silicon substrate decreased at the early stages of metal deposition.

The dependence of the conductance on Fe coverage can be interpreted within the percolation theory [14]. It states that the growth of conductance near the percolation threshold is described by the following expression:

$$\Delta\sigma(d) \propto (d - d_c)^t \text{ for } d > d_c,$$

where  $d_c$  is the critical coverage.

Theoretical estimations given for the case of 2D triangle-shaped islands predict  $d_c = 0.5 \text{ ML}$  and the power factor  $t \approx 1.3$  [15]. Our results give  $t = 1.36 \pm 0.09$

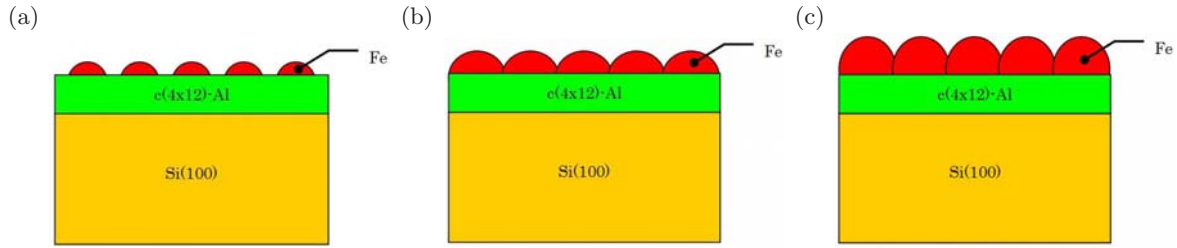


FIG. 9: The stages of iron film growth on the SP Si(100)-c(4×12)-Al at RT. (a) 0-3.7 ML. Nucleation of iron islands and formation of percolation paths of conductance; (b) 3.7-12 ML. Islands' lateral dimensions and height grow resulting in their coagulation; (c) 12-23 ML. The thickness of the continuous film monotonically grows. Highly defective boundaries of the coagulated iron grains remain.

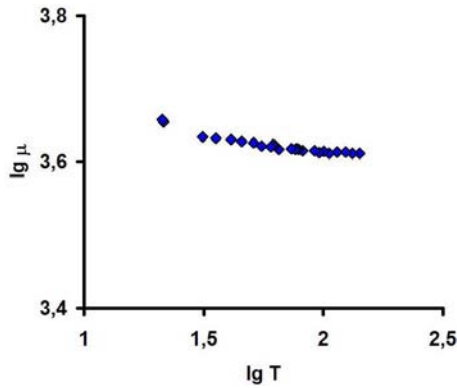


FIG. 10: Hole mobility dependence on temperature for the system 23 ML Fe/Si(100)-c(4×12)-Al/Si.

which satisfactorily agrees with the theory. The critical coverage  $d_c$  (corresponding to beginning of conduction through percolation paths in the ensemble of iron islands) in our case is  $3.7 \pm 0.2$  ML. The significant difference of this value with the theory prediction is the consequence of 3D but not 2D character of Fe island growth. The results obtained for other systems also demonstrate that the critical coverage is always higher than the theory estimations give [16]. In spite of this discrepancy, the good agreement of the factor  $t$  with the theoretical value allows to state that at the early stages of Fe deposition the conductance is supported through the percolation paths.

After the islands grew enough to form a continuous film at  $d_{\text{Fe}} = 12$  ML the conductance linearly increases with iron coverage. This increase can be explained by growth of thickness of the film. This is naturally expressed by the equation  $\Delta\sigma(d) = a \cdot d + b$ , where  $d$  is the film thickness,  $a$  and  $b$  are constants. The factor  $a$  represents the conductivity of the material. From the slope of the linear function it was found that the conductivity is  $1 \times 10^4$  ohm $^{-1}$ cm $^{-1}$  which is one order of magnitude lower than that for bulk iron. This discrepancy is explained by carrier scattering on the highly defective boundaries of the coagulated iron grains.

Atomic force image of the sample with 23 ML iron deposited upon the prefabricated SP Si(100)-c(4×12)-Al is presented in Fig. 8(a). Numerous islands are seen whose density is about  $2 \times 10^{10}$  cm $^{-2}$ . The islands have roundish or oval shape, with average diameter 60 nm and height

4.5 nm (obtained from the histogram given in Fig. 8(b)).

Taking into account that the islands have the sphere segment shape, the estimation for the amount of iron they contain is about 7 ML, i.e. 1/3 of the total material deposited. Hence, under the islands there must exist a layer of polycrystalline iron conducting the current.

Basing on the electric measurements for the disordered iron layers grown on the SP Si(100)-c(4×12)-Al and the AFM data, we come to the following growth model:

At the first stage of deposition (0-3.7 ML) nucleation of iron islands and formation of percolation paths of conductance takes place. Intermixing of iron atoms with substrate is blocked by the prefabricated SP Si(100)-c(4×12)-Al representing a diffusion barrier (Fig. 9(a)). The systems' conductivity is practically constant at this stage. The LEED spots characteristic for the SP Si(100)-c(4×12)-Al can be seen for  $d_{\text{Fe}} \leq 1$  ML. Thus, we conclude that the SP preserves up to the coverage of 1 ML. At the second stage of deposition (3.7-12 ML—see Fig. 9(b)) the islands' lateral dimensions and height grow resulting in their coagulation and increasing of the film's continuousness. This arising conducting channel causes the sharp rise of the effective conductance of the system. At the third stage (12-23 ML) the thickness of the continuous film monotonically grows (Fig. 9(c)). The conductance linearly depends on the amount of the deposited iron.

After completion of the iron deposition, the dependencies of  $U_H$  and  $U_p$  on temperature were measured. The dependence of carrier mobility obtained from this data in the logarithm scale is presented in Fig. 10. The slope of this curve is nearly zero (exponent  $\alpha = -0.05$ ) which indicates scattering on neutral impurities or defects—most probably inter-grain boundaries resulting from iron island coagulation.

## V. CONCLUSIONS

1. The SP Si(100)-c(4×12)-Al formed on *p*-type Si(100) substrate represents a diffusion barrier blocking intermixing of deposited iron atoms with the silicon substrate at RT.
2. The conductance of the iron film deposited on the SP Si(100)-c(4×12)-Al is well described by the percolation theory within the coverage range 0-10 ML. This conductance begins at the coverage 3.7 ML.

3. The main carriers in the system SP Si(100)-c(4×12)-Al/*p*-type boron-doped Si(100) are holes. Conductance and hole mobility in this system are higher than those in clean silicon within the temperature range from RT up to 180°C.
4. Conductance through the continuous iron film begins at the coverage of 12 ML and 20 ML for the film growth on the SP Si(100)-c(4×12)-Al and clean Si(100) surface, respectively.
5. Deposition of  $d_{\text{Fe}} \leq 25$  ML on Si(100)2×1 surface

results in decrease of the effective conductance of the system Fe film/Si(100) substrate.

#### Acknowledgments

This study was supported by the grant of Russian Foundation for Basic Research No. 07-02-00958\_a. The authors are grateful to E. A. Chusovitin for registration of AFM images.

- 
- [1] R. Klasges, C. Carbone, W. Eberhardt, C. Pampuch, O. Rader, T. Kachel, and W. Gutat, *Phys. Rev. B* **56**, 10801 (1997).
  - [2] J. Alvarez, J. J. Hinarejos, E. G. Michel, G. R. Castro, and R. Miranda, *Phys. Rev. B* **45**, 14042 (1992).
  - [3] P. Ma, G. W. Anderson, and P. R. Norton, *Surf. Sci.* **420**, 134 (1999).
  - [4] B. Heinrich, J. A. C. Bland (Eds.), *Ultrathin Magnetic Structures II* (Springer, Berlin, 1994).
  - [5] M. Naitoh, F. Shoji, and K. Oura, *Surf. Sci.* **242**, 152 (1991).
  - [6] K.-H. Park, J. S. Ha, W. S. Yun, and E.-H. Lee, *Surf. Sci.* **415**, 320 (1998).
  - [7] P. Bertoncini, D. Berling, P. Wetzel, A. Mehdaoui, B. Loegel, G. Gewinner, C. Ulhaq-Bouillet, and V. Pierron-Bohnes, *Surf. Sci.* **454**, 755 (2000).
  - [8] N. G. Galkin, D. L. Goroshko, S. A. Dotsenko, A. S. Gouralnik, and I. V. Louchaninov, *Thin Solid Films* **464-465**, 18 (2004).
  - [9] S. Itou, A. Nishida, Y. Murata, O. Kubo, H. Okado, M. Katayama, A. A. Saranin, A. V. Zotov, and K. Oura, *Surf. Sci.* **565**, 121 (2004).
  - [10] N. G. Galkin and D. L. Goroshko, *Phys. Low-Dim. Struct.* **9-10**, 67 (2001).
  - [11] I. Shiraki, F. Tanabe, R. Hobara, T. Nagao, and S. Hasegawa, *Surf. Sci.* **493**, 633 (2001).
  - [12] M. V. Gomoyunova, D. E. Malygin, I. I. Pronin, A. S. Voronchikhin, D. V. Vyalikh, and S. L. Molodtsov, *Surf. Sci.* **601**, 5069 (2007).
  - [13] M. V. Lavrinaitis, D. V. Gruznev, D. A. Tsukanov, and S. V. Ryzhkov, *Tech. Phys. Lett.* **31**, 1068 (2005).
  - [14] D. Stalifter and A. Aharony, *Introduction to Percolation Theory* (Taylor and Francis, London, 1992).
  - [15] M. Sahimi, *J. Phys. A - Math. Gen.* **17**, L601 (1984).
  - [16] S. Hasegawa, X. Tong, S. Takeda, N. Sato, and T. Nagao, *Prog. Surf. Sci.* **60**, 89 (1999).